Asian Journal of Chemistry; Vol. 38, No. 8 (2026), 2067-2075
ASIAN JOURNAL OF CHEMISTRY
https://doi.org/10.14233/ajchem.2026.36156

Synthesis and Optimisation of Glyceryl Monosterate Coated Solid Lipid Nanoparticle of *Asparagus racemosus* Petroleum Ether Extract: Characterisation and *in vitro* Therapeutic Potential

H.K. SUNDEEP KUMAR[1], JITENDRA DEBATA[2], VEERESH YADAV[3] and SANDIP SEN[4,*]

[1]Department of Pharmaceutical Chemistry, Institute of Pharmacy and Technology Salipur, Cuttack-754202, India
[2]Department of Pharmaceutical Chemistry, Bengal College of Pharmaceutical Technology, Dubrajpur, Birbhum-731123, India
[3]Keva Fragrances Pvt. Ltd. Plot No. 170, GIDC, Vapi-396195, India
[4]Department of Pharmaceutical Chemistry, School of Pharmacy, Guru Nanak Institutions Technical Campus, Khanapur, Ibrahimpatnam-501506, India

*Corresponding author: E-mail: sandipsen2010@gmail.com

Received: 6 April 2026 *Accepted*: 27 June 2026 *Published online*: 7 August 2026 AJC-22433

The therapeutic potential of *Asparagus racemosus* arises from its diverse phytoconstituents; however, the petroleum ether extract contains comparatively fewer phytochemicals since it primarily extracts non-polar constituents. To improve the bioavailability and therapeutic efficacy of this extract, glyceryl monostearate-coated solid lipid nanoparticles (SLNs) were synthesised using the non-ionic surfactant Tween 80. Plant extraction was carried out using a Soxhlet apparatus with petroleum ether as the extraction solvent and the potential bioactive compounds were identified by GC-MS analysis. Glyceryl monostearate-coated solid lipid nanoparticles (SLNs) were prepared by the reverse-phase solvent evaporation method, followed by spectral, morphological, thermal characterisation and subsequently evaluated for *in vitro* drug release, antioxidant, anti-inflammatory and diuretic activities in comparison with the crude extract. The compound pregnane-3,20β-diol,14α,18α-[4-methyl-3-oxo-(1-oxa-4-azabutane-1,4-diyl)]-diacetate exhibited the highest relative abundance, accounting for 37.33% of the total peak area in the GC-MS chromatogram. The optimised SLNs has mean particle size of 104.0 ± 8.01 nm, zeta potential -40.09 ± 7.5 mV and a polydispersity index (PDI) value of 0.33. The particle size revealed non-uniform, spherical particles with nanoscale formulation and structural integrity was confirmed by microscopic study. FTIR and thermal analyses confirmed the chemical compatibility of the formulation components and its good thermal stability. The optimised SLN formulation (1:1:1) exhibited sustained drug release and superior therapeutic efficacy compared with the crude extract, which may be attributed to improved permeability of the major steroidal alkaloid.

Keywords: *Asparagus racemosus*, Solid lipid nanoparticles, Glyceryl monosterate, Particle size distribution, *In vitro* studies.

INTRODUCTION

In the Ayurvedic system, *Asparagus racemosus* Willd., of the family Asparagaceae, reflects its long-standing reputation for enhancing female reproductive health and vitality. Traditionally, the plant has been employed as a rejuvenating tonic, aphrodisiac and lactation enhancer. The roots are rich in biologically active non-polar constituents such as steroids, lignans and terpenoids, which contribute to their therapeutic properties [1].

Pharmacological investigations have demonstrated that *A. racemosus* (Shatavari) possesses potent anti-inflammatory, antioxidant, anti-ulcer and immunomodulatory activities. Its ability to attenuate stress-induced physiological responses has frequently been compared with that of *Panax ginseng* [2]. Clinically, the plant has exhibited a favourable therapeutic profile in the management of female reproductive disorders, such as menopausal symptoms, premenstrual syndrome and inadequate lactation [3]. Evidence from randomized controlled trials has further validated its galactagogue activity [4]. The mucilaginous nature of the roots, together with their antioxidant properties, has been associated with improved gastric ulcer healing [5,6]. Immunological investigations have reported enhanced phagocytic activity and lymphocyte proliferation, supporting the immune-enhancing properties of the plant. These diverse pharmacological attributes have stimulated increasing interest in the incorporation of Shatavari into contemporary herbal formulations and functional food products [7].

Despite these therapeutic advantages, many bioactive phytochemicals present in plant extracts undergo degradation or reduced efficacy under the harsh conditions of the gastrointestinal environment. Solid lipid nanoparticles (SLNs) have emerged as an attractive delivery system due to their high surface area-to-volume ratio, superior physico-chemical stability and improved gastrointestinal resilience. These nanocarriers have found wide application in drug delivery, biomedical diagnostics [8], targeted drug delivery (TDD) and photothermal therapy owing to their favourable functional characteristics [9].

The novelty of the present study lies in the development and optimisation of an SLNs formulation containing *A. racemosus* extract with improved physico-chemical properties and enhanced biological performance. The therapeutic potential of the optimised formulation was evaluated through *in vitro* antioxidant, anti-inflammatory and diuretic assays and compared with that of the crude extract. The present work contributes formulation-specific data that are currently lacking in the literature. The novelty of the study lies in the optimisation of the SLN formulation of *A. racemosus* extract to improve its biological performance, rather than in the introduction of a new nanocarrier platform.

EXPERIMENTAL

Collection of plant material and extraction: Fresh stems material of *A. racemosus* were collected from Ibrahimpatnam, India (16.5811ºN, 77.7489ºE; 373 m above mean sea level). The plant material was botanically authenticated by the Department of Botany, Osmania University, Hyderabad, India.

Preparation of extract: The shade-dried stem powder (300 g) was subjected to Soxhlet extraction using petroleum ether (1 L; boiling range 60 ºC) as the extraction solvent. The powdered material was packed in a 100-mesh muslin cloth and extracted until the solvent in the siphon tube became colourless. The extract was concentrated under reduced pressure using a rotary evaporator (Rotavapor R-300, Büchi, India) at 65 ºC and 50 rpm. The concentrated residue was subsequently dried in a desiccator to a constant weight and the percentage yield was calculated [10].

Phytochemical screening: Qualitative phytochemical analysis of the extract was conducted following standard literature protocols to identify the presence of bioactive secondary metabolites [11].

GC-MS analysis: Agilent 7890A GC System assembled Mass Spectrometer The AccuTOFGCv/JMS-T100GCv made of JEOL was used for GC-MS analysis. The petroleum ether extract (30 µg/mL) was used for analysis. The sample was eluted out using an HP5 Column having a dimension of 30 m × 0.25 mm × 0.25 µ. The carrier gas helium was supplied at a flow rate of 1 mL/min. During analysis oven temperature was maintained at 280 ºC. The isolated compounds were recognised by comparing their mass spectra in the NIST library database.

Synthesis of solid lipid nanoparticles (SLNs): The SLNs was prepared by ether injection method. In a round bottom flask, 1 g of glyceryl mono sterate and varying amount of Tween 80 (Table-1) was dissolved in 50 mL of chloroform. In 50 mL conical flask, 1 g of extract was dissolved in 20 mL of phosphate buffer (pH 7.4). The ether mixture was mixed with aqueous phase at a rate of 2.0 mL/min using a Remi magnetic stirrer 2MLH from Mumbai, India. The resulting mixtures were refluxed for 1 h at 60-65 ºC with constant stirring. The organic phase was eliminated using a rotary flash evaporator (Cyberlab Corporation, CR2001, India) operating at 65 ºC and 50 rpm. The aqueous phase was homogenised for 2 h at 8000 rpm (Remi homogenizer, RQT-1275, Mumbai, India). The mixtures were sonicated at 10 ºC for 30 min at 30 sec intervals (Citizen Digital ultrasonicator, CD4820). The formulation was kept between 2 ºC and 8 ºC in a brown glass container until it was evaluated.

TABLE-1
COMPOSITION OF SLNs

Ingredients (g)	GSP1	GSP2	GSP3	GSP4	GSP5
Extract	1	1	1	1	1
GMS	1	1	1	1	1
Tween 80	0.25	0.50	0.75	1	1.25

Characterisation: The morphology of the solid lipid nanoparticles (SLNs) was examined by environmental scanning electron microscopy (ESEM) using an FEI Quanta 200 microscope (Hillsboro, USA). Two drops (40 µL) of the sample were placed on conductive copper tape, air-dried, sputter-coated with a 10 nm platinum layer, and imaged at a magnification of 2500×. The average particle diameter was determined using ImageJ software. The transverse morphology of the SLNs was further evaluated by transmission electron microscopy (TEM) using a JEM-2100F microscope (Tokyo, Japan). A drop of the SLNs suspension was deposited onto a 200-mesh carbon-coated copper grid, excess solvent was removed with filter paper and the samples were air-dried before imaging. The average particle diameter was determined using ImageJ software. Fourier-transform infrared (FTIR) spectroscopy was performed using a Bruker Vertex-80 spectrometer (Germany) equipped with a Hyperion-3000 microscope. Approximately 1 mg of the extract and 1 mL of the SLNs dispersion were analysed in Micro-ATR mode over the spectral range of 4000-450 cm^{-1}. Thermal stability and weight-loss behaviour were investigated using a Hitachi NEXTA STA-300 simultaneous thermogravimetric analyser. Approximately 28.34 mg of each sample was placed in a ceramic crucible and heated from 30 to 800 ºC at a heating rate of 10 ºC/min under a nitrogen atmosphere.

Entrapment efficiency: The entrapment efficiency of the *A. racemosus* petroleum ether extract-loaded SLNs was determined indirectly by quantifying the free steroidal constituents present in the supernatant using the Liebermann–Burchard colorimetric method. An aliquot (1 mL) of the SLNs dispersion was centrifuged at 15,000-20,000 rpm for 30-45 min using a refrigerated centrifuge to separate the unentrapped extract from the nanoparticles. The supernatant containing the free steroidal constituents was carefully collected and analysed by the Liebermann–Burchard method. An appropriate volume of the supernatant was mixed with chloroform, followed by the addition of 2 mL of acetic anhydride and 0.2 mL of concentrated sulfuric acid. After incubation in the dark for 15 min, the absorbance was recorded at 630 nm using a UV-visible spectrophotometer (Labman LMSPUV-

1920). The concentration of free steroidal constituents was determined from a β-sitosterol calibration curve and expressed as β-sitosterol equivalents [12]. The results are presented as mean ± standard deviation. The entrapment efficiency (%EE) was calculated using the following equation:

$$EE\ (\%) = \frac{C_1 - C_2}{C_1} \times 100$$

where C_1 = concentration of β-sitosterol equivalents loaded; C_2 = concentration of free β-sitosterol equivalents found in supernatant. All measurements were performed in triplicate and the results were expressed as mean ± standard deviation.

Particle size, zeta potential and PDI: Particle size distribution, polydispersity index (PDI) and zeta potential were evaluated using a Malvern Zetasizer (Malvern Instruments, UK). Measurements were conducted at 25 ± 2 ºC with a scattering angle of 90º. Refractive index and absorption values were set at 1.330 and 0.050, respectively. Zeta potential measurements were performed using an electrode cuvette. All analyses were conducted in triplicate.

***In vitro* drug release study:** The diffusion method was used for the *in vitro* drug release study. The USP Dissolution Tester (TDT-08L, Electrolab, India) filled with 900 mL of phosphate buffer (pH 6.8) and maintained 37.5 ± 0.5 ºC. A pretreated dialysis membrane (Dialysis Membrane-60, flat width: 25.27 mm, average diameter: 15.9 mm, capacity approximately 1.99 mL/cm, Mumbai, India), contained 5 mL of the formulation (equivalent to 250 mg extract) was agitated at 50 rpm. To maintain sink conditions, 5 mL samples were replaced with new buffer at prearranged intervals. UV spectroscopic method was used to quantify drug release. The % CDR was computed. Zero-order, first-order, Higuchi and Korsmeyer-Peppas models were used to examine release kinetics; the model with the highest correlation coefficient (R^2) was deemed to be the best fit. The results are shown as mean ± standard deviation and each experiment was conducted in triplicate.

***In vitro* antioxidant activity:** The antioxidant activity of the extract, optimised SLN formulation (GSP4) and the standard was evaluated using the DPPH free radical scavenging assay [13]. Test solutions were prepared at concentrations of 25, 50, 75, 100 and 125 µg/mL. To each sample, 2 mL of 0.004% DPPH solution was added, followed by incubation in the dark for 30 min to allow completion of the reaction. The absorbance was recorded at 517 nm using a UV-visible spectrophotometer. The free radical scavenging activity was expressed as percentage inhibition and the IC_{50} value was determined for each sample. The IC_{50} values were used for the determination of fold improvement in comparison to extract.

$$\text{Inhibition}\ (\%) = \frac{Abs_{control} - Abs_{test}}{Abs_{control}} \times 100$$

$$\text{Fold improvement} = \frac{IC_{50}\ \text{of extract}}{IC_{50}\ \text{of SLNs}}$$

***In vitro* anti-inflammatory activity:** The anti-inflammatory activity of the extract and the optimised SLNs formulation (GSP4) was evaluated using modified albumin denaturation inhibition, anti-proteinase and anti-lipoxygenase assays as described earlier [14]. Test solutions of the extract, GSP4, standard drugs (diclofenac sodium and indomethacin), and the control were prepared at concentrations ranging from 25 to 100 µg/mL. For each assay, 1 mL of the test or standard solution was mixed with 9 mL of the respective working reagent and the procedures were carried out according to the corresponding assay protocol [15]. Albumin denaturation inhibition was assessed to evaluate the anti-inflammatory potential of the samples. Briefly, 1 mL of 1% (w/v) bovine serum albumin was mixed with the test sample, diclofenac (standard) or control. The pH was adjusted to 6.3, followed by incubation at 37 ºC for 30 min and heating at 70 ºC for 5 min to induce protein denaturation. After cooling, the absorbance was recorded at 660 nm.

The anti-proteinase assay was performed to assess the inhibition of proteolytic enzymes associated with inflammatory tissue damage. Briefly, 1 mL of 1% Tris-HCl buffer (pH 7.4-7.8) was mixed with the test sample, diclofenac (standard) or control and incubated at 37 ºC for 5 min. Subsequently, 1 mL of 1% casein was added, followed by incubation for 20 min. The reaction was terminated with perchloric acid, centrifuged and the absorbance of the supernatant was recorded at 210 nm [15].

The anti-lipoxygenase assay was carried out to evaluate the inhibition of lipoxygenase, an enzyme involved in the formation of inflammatory mediators such as leukotrienes. The test sample, indomethacin (standard) or control was incubated with the enzyme for 5 min at room temperature, followed by the addition of 1 mL of 5% linoleic acid. The absorbance was measured at 234 nm [15]. For both assays, the percentage inhibition and IC_{50} values were calculated. The IC_{50} values were used to determine the fold improvement of the SLNs formulation relative to the extract.

$$\text{Inhibition}\ (\%) = \frac{Abs_{control} - Abs_{test}}{Abs_{control}} \times 100$$

***In vitro* diuretic activity (electrolyte ion estimation):** The *in vitro* diuretic activity of the extract and the optimised SLNs formulation (GSP4) was evaluated by a spectrophotometric method using spironolactone as the standard [16]. Test solutions of the extract, GSP4 and spironolactone were prepared at concentrations of 50, 75 and 100 µg/mL, while phosphate buffer (pH 7.4) served as the control. Briefly, 5 mL of buffer solution was mixed with 1 mL of the respective test or standard solution. The electrolyte-specific reagents were then added: sodium magnesium uranyl acetate for sodium (Na^+), sodium tetraphenylborate for potassium ions and mercuric thiocyanate with ferric nitrate for chloride ions. The reaction mixtures were allowed to stand for 10-15 min for colour development and incubated at 37 ºC for 60 min. The absorbance was measured using a UV-visible spectrophotometer at 540, 620 and 480 nm for Na^+, K^+ and Cl^-, respectively. The electrolyte concentrations were determined from calibration curves prepared using standard electrolyte solutions, and the diuretic activity of the extract and GSP4 was evaluated by comparison with the control and spironolactone (standard).

$$\text{Diuretic activity (DA)} = \frac{[\text{Ion in test}]}{[\text{Ion in standard}]}$$

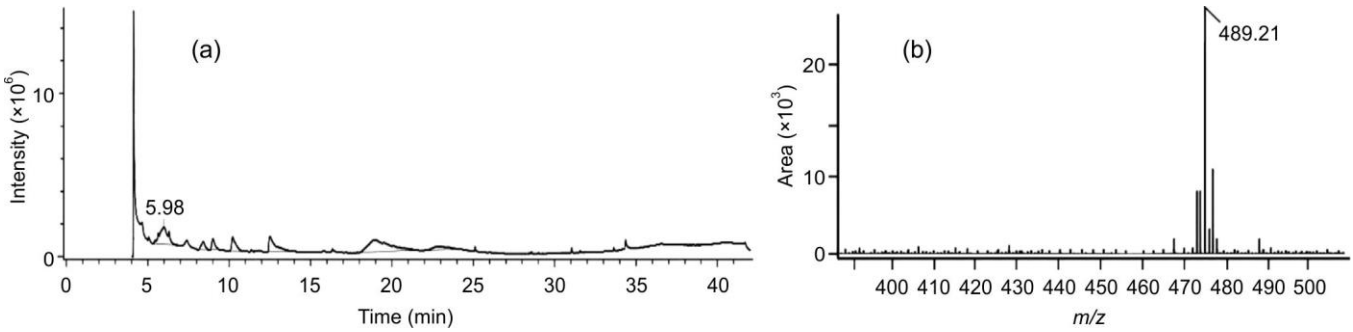

Fig. 1. LC-MS analysis of the reported compound: (a) total ion chromatogram and (b) corresponding mass spectrum

$$\text{Diuretic index} = \frac{[\text{DA of test}]}{[\text{DA of standard}]}$$

Statistical analysis: All experiments were performed in triplicate, and the results are presented as mean ± standard deviation (SD). Statistical analysis was carried out using GraphPad Prism version 8.0.2 (GraphPad Software, San Diego, USA). Differences among groups were analysed by one-way analysis of variance (ANOVA), followed by Dunnett's post hoc test to compare the treatment groups with the control. A $p \leq 0.05$ was considered statistically significant.

RESULTS AND DISCUSSION

The GC-MS chromatograms of the petroleum ether extract are shown in Fig. 1. Seven compounds were identified, with pregnane-3,20β-diol,14α,18α-[4-methyl-3-oxo-(1-oxa-4-aza-butane-1,4-diyl)]-diacetate being the major constituent, accounting for 37.33% of the total peak area at a retention time of 19.02 min. The identity of the compounds was confirmed by mass spectrometry. This steroidal alkaloid may account for the antioxidant, anti-inflammatory and diuretic activities of the extract through glucocorticoid receptor activation and mineralocorticoid receptor blockade [10].

Development of formulations: Solid lipid nanoparticles (SLNs) containing the petroleum ether extract were prepared by the ether injection method and their compositions are listed in Table-1. The major phytoconstituent possesses poor aqueous solubility, a low distribution coefficient and limited oral bioavailability, which may restrict its therapeutic application. To improve these properties, SLNs were formulated using glyceryl monostearate as the lipid and Tween 80 as the surfactant [17]. The SLNs remained stable at physiological pH (7.2). The high-speed homogenisation at 10,000 rpm yielded nanosized particles. A lipid:surfactant:extract ratio of 1:1:1 (w/v) provided the most stable formulation.

Entrapment efficiency: Entrapment efficiency (%EE) increased with surfactant concentration and reached a maximum at the 1:1:1 ratio because of the optimal particle stabilisation. The EE ranged from 56.33 ± 1.75% to 91.50 ± 1.64% (Fig. 2). Increasing the lipid concentration improved EE, while excess surfactant reduced the EE of formulation GSP5 to 86.83 ± 1.47%. Lower surfactant levels resulted in poor encapsulation, whereas higher concentrations caused slight drug leakage. Higher lipid content influenced particle size, surface morphology and drug release kinetics through stronger lipid–drug interactions.

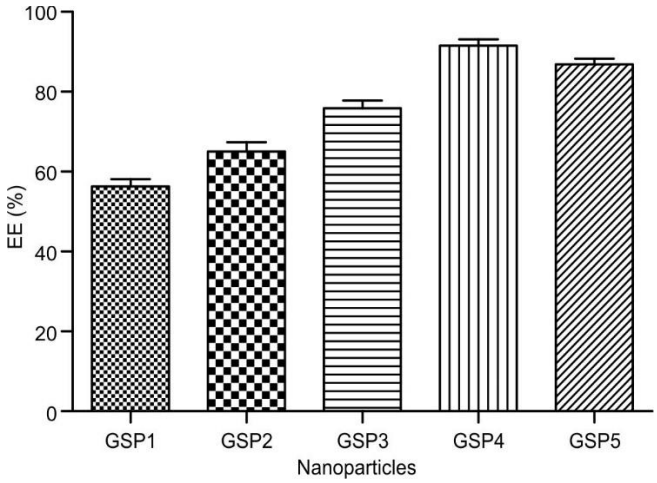

Fig. 2. Entrapment efficiency (%) of GSP-loaded SLNs prepared using different formulations

Particle size distribution and zeta potential: Particle size distribution and zeta potential values are summarised in Table-2. Lipid and surfactant concentrations markedly influenced particle size, surface charge and colloidal stability [18]. Increasing the lipid concentration increased particle size, zeta potential and polydispersity. At the highest lipid concentration (1.25 g), both colloidal stability and particle size uniformity declined. Formulation GSP4 exhibited a mean particle size of 104.0 ± 8.01 nm, a zeta potential of -40.09 ± 7.5 mV and a polydispersity index (PDI) of 0.33 (Fig. 3). The high negative zeta potential reflects good electrostatic stability, while the PDI of 0.33 indicates an acceptable and moderately uniform particle size distribution. Particle size decreased as the surfactant concentration increased up to the 1:1:1 ratio due to the improved interfacial stabilisation, accompanied by a lower PDI.

TABLE-2
PARTICLE SIZE DISTRIBUTION AND ZETA POTENTIAL OF GSP-LOADED SLNS

Formulation	Z average (d.nm) ± SD	Zeta potential (mV) ± SD	PDI
GSP1	100.2 ± 7.5	-18.1 ± 7.2	0.25
GSP2	101.4 ± 8.1	-25.2 ± 6.4	0.28
GSP3	102.5 ± 9.2	-31.02 ± 5.1	0.31
GSP4	104.2 ± 8.1	-40.09 ± 7.5	0.37
GSP5	107.3 ± 7.3	-22. ± 7.1	0.47

All the studies carried out in triplicate and data are represented in Mean ± SD

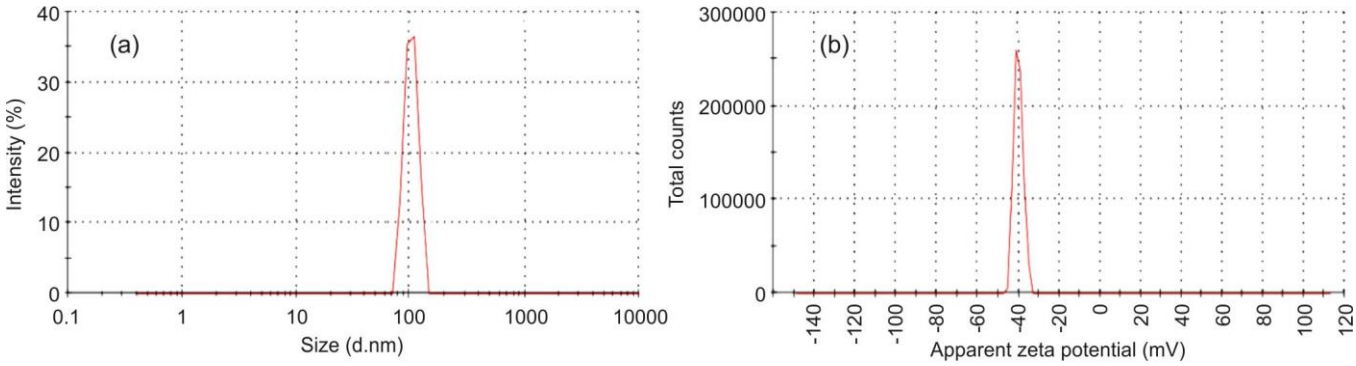

Fig. 3. Particle size and zeta potential distributions of GSP4-loaded solid lipid nanoparticles (SLNs)

Morphological studies: The ESEM and TEM micrographs (Fig. 4a-b) revealed predominantly spherical SLNs with average particle sizes of 138 and 100.34 nm, respectively, confirmed the nanoscale dimensions and structural integrity of the formulation [12]. Formulations containing an intermediate Tween 80 concentration exhibited well-defined spherical particles, whereas lower or higher surfactant concentrations resulted in irregular morphologies [19].

The particle sizes obtained by DLS (104.0 ± 8.01 nm), ESEM (138 nm) and TEM (100.34 nm) were in good agreement. The slightly larger particle size measured by ESEM may be attributed to particle aggregation during sample drying, while the close agreement between DLS and TEM confirms a moderately uniform particle size distribution with minimal aggregation. These observations are consistent with the low PDI (0.33) and high negative zeta potential (-40.09 ± 7.5 mV), which reflect good colloidal stability of the optimised formulation.

FTIR analysis and Voigt deconvolution: The FTIR spectra of the plant extract, excipients and the optimised formulation (GSP4) were analysed using Voigt profile deconvolution to evaluate compatibility and intermolecular interactions. The plant extract exhibited characteristic absorption bands at 3390 cm^{-1} (O–H *str*.), 2929 cm^{-1} (aliphatic C–H *str*.) and 1638 cm^{-1} (arom. C=C *str*.), which confirmed the presence of phenolic and other phytoconstituents. Glyceryl monostearate (GMS) displayed characteristic bands at 2940-2917 cm^{-1} (methylene C–H *str*.) and 1735 cm^{-1} (ester C=O *str*.), while Tween 80 exhibited peaks at 3390 cm^{-1} (O–H *str*.), 2950-2850 cm^{-1} (C–H *str*.), 1735 cm^{-1} (ester C=O cm^{-1}) and 1100-1000 cm^{-1} (C–O–C *str*.). The optimised formulation retained the characteristic absorption bands of both the extract and excipients, with a slight shift of the O–H stretching band to 3435 cm^{-1}, attributed to hydrogen bonding [20]. No new absorption bands were detected, further approved the absence of chemical incompatibility among the formulation components. The minor peak shifts are consistent with weak non-covalent interactions, which may improve the stability of the SLNs (Fig. 5).

Thermal studies: The TG thermogram of the optimised SLNs (Fig. 6a) exhibited a multistep degradation pattern. An initial weight loss of 1.2% (0.36 mg) below 100 ºC was attributed to the removal of adsorbed moisture and residual solvents. A second stage between 100 and 280 ºC resulted in an 8.6% (2.58 mg) weight loss, corresponding to the decomposition of surfactants and other volatile constituents. The major degradation event occurred between 280 and 450 ºC, with a 64.7% (19.41 mg) weight loss arising from decomposition of the

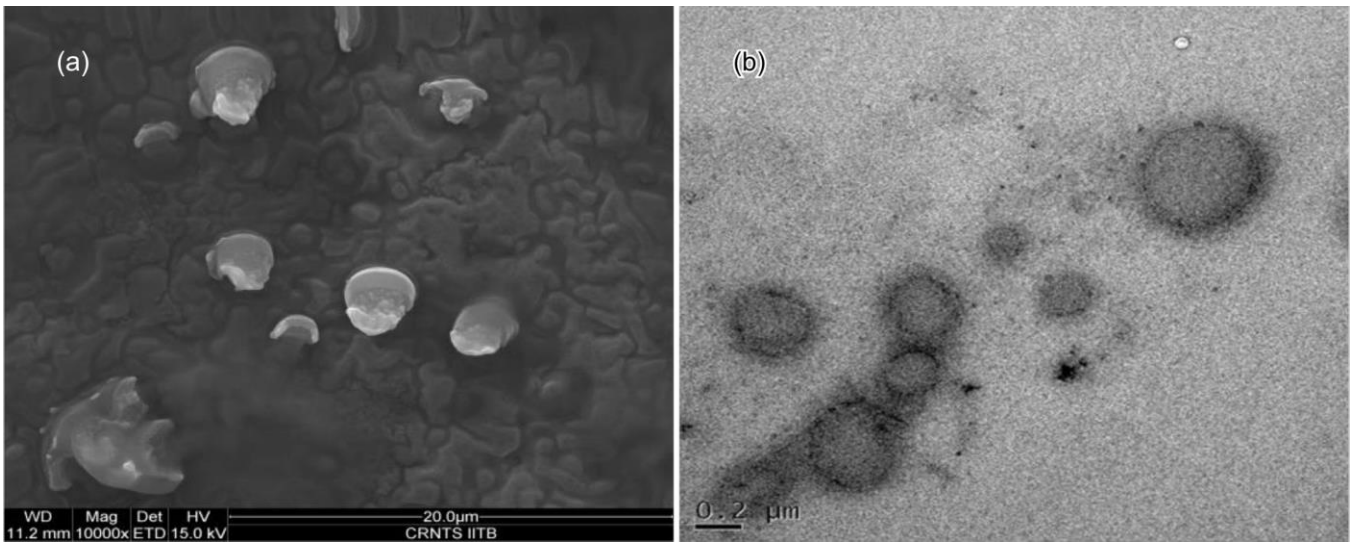

Fig. 4. Morphological images of GSP4 phytosomes by (a) environmental scanning electron microscopy (ESEM) and (b) high-resolution transmission electron microscopy (HRTEM)

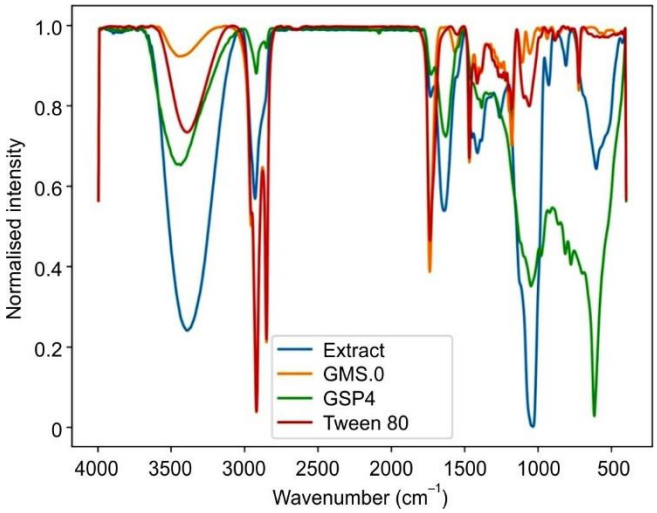

Fig. 5. Overlay FTIR spectra of extract, lipid, surfactant and SLNs GSP4

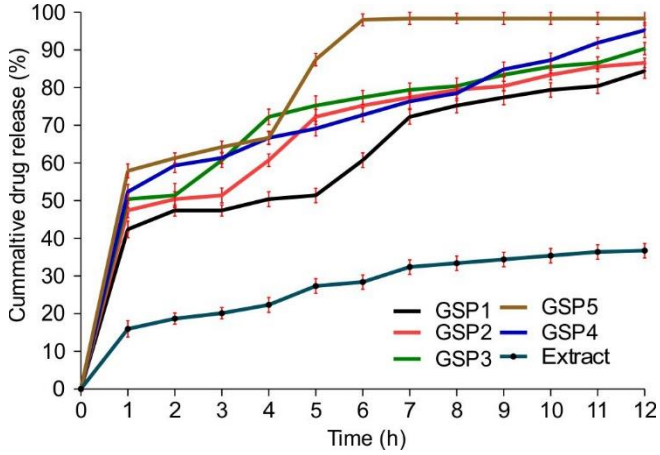

Fig. 7. *In vitro* release profiles of SLNs

lipid matrix. Gradual degradation continued up to 800 ºC, leaving a residual mass of 4.8%. These results indicate that the SLNs remain thermally stable up to approximately 250-280 ºC before extensive degradation occurs.

The DTA thermogram (Fig. 6b) displayed a minor endothermic peak near 60 ºC due to moisture loss, followed by an endothermic transition at approximately 220 ºC associated with lipid phase rearrangement. A prominent exothermic peak around 340 ºC corresponded to thermal degradation of the lipid matrix, while a second exothermic event near 480 ºC was attributed to the decomposition of residual carbonaceous material. The thermal behaviour confirms good stability and preservation of the SLNs structure up to temperatures exceeding 300 ºC [21].

***In vitro* release study:** The *in vitro* drug release profiles are shown in Fig. 7. All SLNs formulations exhibited a biphasic release pattern characterised by an initial burst release followed by sustained drug release. The initial release ranged from 42.39 ± 2.17% (GSP1) to 57.92 ± 1.87% (GSP5), while the pure extract exhibited substantially lower release throughout the study. After 12 h, the cumulative drug release reached 83.39 ± 1.93% (GSP1), 86.58 ± 1.29% (GSP2), 90.37 ± 1.64% (GSP3), 95.24 ± 1.91% (GSP4), and 98.38 ± 1.48% (GSP5), compared with only 36.73 ± 1.93% for the extract due to its poor aqueous solubility. Increasing the surfactant concentration enhanced both the initial burst release and cumulative drug release by improving drug dispersion and reducing the interfacial tension between the lipid and aqueous phases. Formulation GSP5 exhibited the fastest release, reaching near-complete drug release within 6 h. In contrast, GSP4 provided a more controlled and sustained release over the entire 12 h study, making it the most suitable formulation for prolonged drug delivery [22].

Drug release kinetics: The drug release kinetics of the optimised formulation (GSP4) were evaluated by fitting the *in vitro* release data to zero-order, first-order, Higuchi and Korsmeyer-Peppas models using Microsoft Excel (Fig. 8). Among the kinetic models, the Higuchi model exhibited the highest correlation coefficient (R^2 = 0.967), identifying it as the best fit for the release data. This finding indicates that drug release was primarily governed by diffusion through the lipid matrix. The Korsmeyer-Peppas release exponent (n = 0.503) indicates anomalous (non-Fickian) transport, where drug release is controlled by a combination of diffusion and matrix relaxation [23].

***In vitro* antioxidant activity:** The DPPH free radical scavenging activity is shown in Table-3. The percentage inhibition increased in a concentration-dependent manner, reaching 89.12 ± 0.26% for the extract, 97.28 ± 0.34% for GSP4-SLNs and 98.10 ± 0.18% for ascorbic acid. The highest anti-

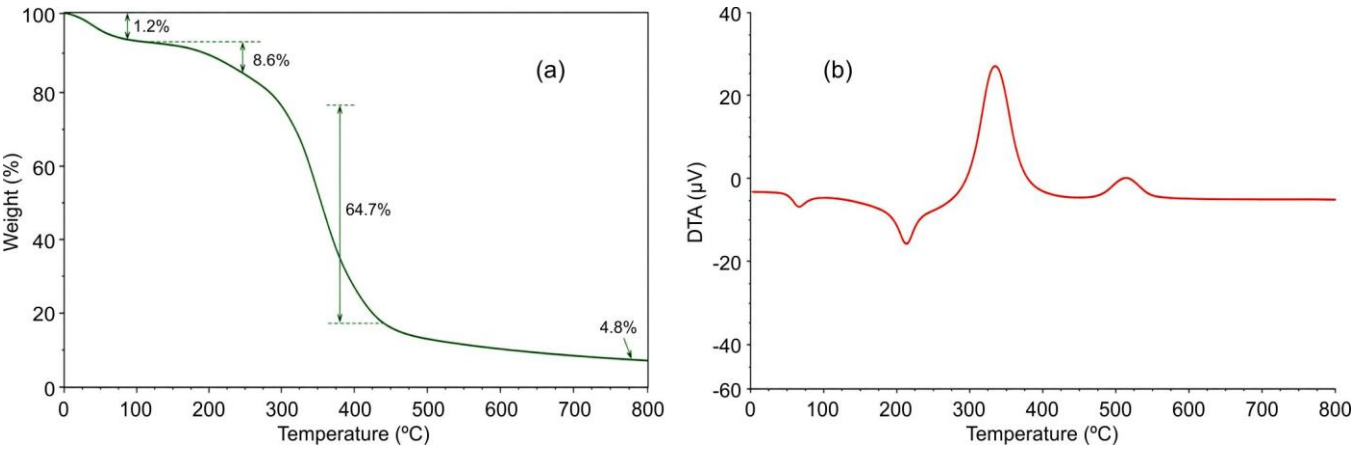

Fig. 6. TGA (a) and DTA (b) curves of SLNs GSP4

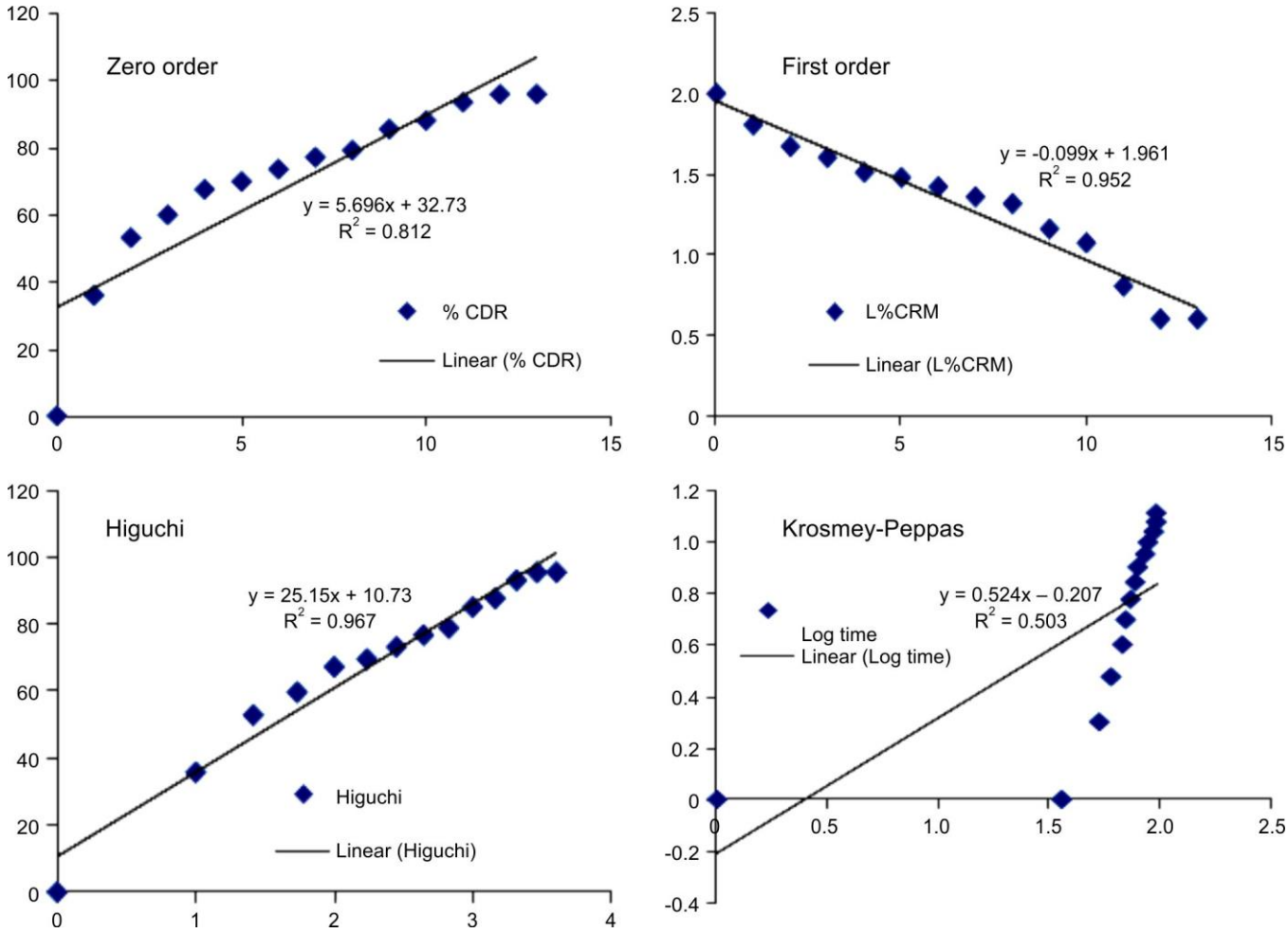

Fig. 8. *In vitro* release kinetics of the optimised SLNs GSP4

TABLE-3
ANTIOXIDANT ACTIVITY OF EXTRACT AND GSP-LOADED SLNS EVALUATED BY THE DPPH RADICAL SCAVENGING ASSAY

Compound	DPPH scavenging effect (%) [mean ± SD]					IC_{50} (µg/mL)
	25 µg/mL	50 µg/mL	75 µg/mL	100 µg/mL	125 µg/mL	
Extract	33.31 ± 0.26*	43.71 ± 0.42*	55.71 ± 0.38*	68.77 ± 0.45**	89.12 ± 0.26**	110.27
SLNs (GSP4)	44.86 ± 0.01**	59.46 ± 0.06**	77.21± 0.45**	82.55 ± 0.12**	97.28 ± 0.34**	86.41
Ascorbic acid	24.28 ± 0.12*	43.03 ± 0.19**	54.06 ± 0.2**	77.02 ± 0.09**	98.10 ± 0.18*	95.72

All the studies carried out in triplicate and data are represented in Mean ± SD. $^{**}p \leq 0.05$ considered as significant in comparison to control group, $^{*}p \geq 0.05$ considered as less significant in comparison to control group.

oxidant activity was observed for the SLN formulation. The IC_{50} values were 110.27 µg/mL for the extract, 86.41 µg/mL for GSP4-SLNs and 95.72 µg/mL for ascorbic acid.

The lower IC_{50} value of GSP4-SLNs represents an approximately 1.28-fold improvement over the crude extract, reflecting enhanced free radical scavenging activity following nanoencapsulation. This improvement may be attributed to increase stability, solubility and bioavailability of the encapsulated phytoconstituents, leading to improved antioxidant efficacy. Similar enhancements have been reported for plant extract-loaded SLNs and other nanoparticle systems, where nanoencapsulation improved the biological performance of phytoconstituents [24].

***In vitro* anti-inflammatory activity:** The *in vitro* anti-inflammatory activity was evaluated by protein denaturation inhibition, anti-proteinase and anti-lipoxygenase assays. The results are shown in Table-4. All samples exhibited concentration-dependent inhibition, with the highest activity observed at 100 µg/mL. In the protein denaturation assay, the percentage inhibition was 82.88 ± 2.84% for the standard, 68.25 ± 1.12% for the extract and 80.29 ± 2.06% for GSP4-SLNs. The anti-proteinase assay yielded inhibition values of 77.88 ± 2.84%, 63.25 ± 1.12% and 75.29 ± 2.06% for the standard, extract and GSP4-SLNs, respectively. In the anti-lipoxygenase assay, the corresponding inhibition values were 76.55 ± 1.99%, 63.25 ± 1.12% and 72.29 ± 2.06%. The SLN formulation consistently exhibited higher anti-inflammatory activity than the crude extract. Based on the IC_{50} values, GSP4-SLNs exhibited 1.36-, 1.20- and 1.09-fold improvements in protein denaturation inhibition, anti-proteinase activity and anti-lipoxy-

TABLE-4
EVALUATION OF *in vitro* ANTI-INFLAMMATORY ACTIVITY OF THE PETROLEUM ETHER EXTRACT AND GSP-LOADED SLNS

Conc. (µg/mL)	Mean ± SD (percentage of inhibition)		
	Standard (ibuprofen)	Petroleum ether extract	SLNs (GSP4)
Protein denaturation			
25	24.36±1.83*	28.08±1.12*	26.04±1.17*
50	37.65±1.99*	43.62±2.06*	45.5±1.69*
75	60.26±1.71*	65.6±1.31*	71.1±2.31**
100	68.25±1.12**	82.88±2.84**	80.29±2.06**
IC_{50} (µg/mL)	59.65	77.98	57.37
Anti-proteinase activity			
25	19.36±1.83*	23.04±1.15*	21.04±1.17**
50	32.65± 1.99*	38.62±2.06*	40.5±1.69**
75	55.26±1.71*	62.27±1.60*	66.1±2.31**
100	63.25±1.12**	77.88±2.84**	75.29±2.06**
IC_{50} (µg/mL)	59.25	69.51	57.77
Anti-lipoxygenase activity			
25	21.04±1.17	27.04±1.15*	16.36±1.83*
50	37.5±1.69	41.62±2.06*	32.65±1.99*
75	63.1±2.31	64.93±1.54**	55.26 ±1.71**
100	72.29±2.06	76.55±1.99**	63.25 ±1.12**
IC_{50} (µg/mL)	58.88	63.17	57.74

All the studies carried out in triplicate and datas are represented in Mean ± SD. $^{**}p \leq 0.05$ considered as significant in comparison to control group, $^{*}p \geq 0.05$ considered as less significant in comparison to control group.

genase activity, respectively, when compared with the petroleum ether extract. The protein denaturation assay exhibited the significant improvement which indicates a significant enhancement in the anti-inflammatory potency of the nano-encapsulated formulation.

***In vitro* diuretic activity:** The *in vitro* diuretic activity was evaluated by the spectrophotometric method and the results are shown in Table-5. Both the petroleum ether extract and GSP4-SLNs exhibited concentration-dependent increases in electrolyte excretion, with the highest activity observed at 100 µg/mL. At this concentration, the diuretic action (DA) values for the standard were 2.50, 2.80 and 2.50 for Na^+, K^+ and Cl^-, respectively. The corresponding DA values for the petroleum ether extract were 2.15, 2.47 and 2.22, whereas GSP4-SLNs exhibited the highest diuretic action with values of 2.75, 3.07 and 2.67. The diuretic indices (DI) of GSP4-SLNs were 1.10, 1.10 and 1.07 for Na^+, K^+ and Cl^-, respectively, compared with 0.86, 0.88 and 0.89 for the extract.

Compared with the petroleum ether extract, GSP4-SLNs exhibited approximately 1.28-fold, 1.25-fold and 1.20-fold higher diuretic indices for Na^+, K^+ and Cl^-, respectively, at 100 µg/mL. The enhanced electrolyte excretion indicates a significant improvement in the diuretic activity of the nano-encapsulated formulation, which may be attributed to the improved solubility, stability and bioavailability of the encapsulated phytoconstituents [25].

Conclusion

This study confirms the therapeutic potential of *Asparagus racemosus* through the identification of a bioactive substituted purine alkaloid and the enhancement of its delivery using a solid lipid nanoparticles (SLNs) formulation. The poor aqueous solubility and limited oral bioavailability of the bioactive compound necessitated formulation optimisation. SLNs prepared using glyceryl monostearate and Tween 80 effectively addressed these limitations. Among the formulations evaluated, the 1:1:1 ratio of phytoconstituent, glyceryl monostearate and Tween 80 exhibited the highest entrapment efficiency, uniformly distributed spherical particles, excellent thermal stability and sustained drug release. The optimised formulation improved solubility, intestinal permeability and the biological performance of the encapsulated phytoconstituents compared with the crude extract. The SLNs formulation significantly enhanced the antioxidant, anti-inflammatory and diuretic activities of *A. racemosus*. The *in vitro* findings provide preliminary evidence supporting the improved biological efficacy of the nanoformulation over the crude extract. Further validation through appropriate *in vivo* studies is required to establish its therapeutic potential and clinical relevance.

ACKNOWLEDGEMENTS

The authors express their sincere thanks to Principal and Management of School of Pharmacy, Guru Nanak Institutions for providing the support. The authors gratefully acknowledge

TABLE-5
EFFECT OF EXTRACT AND GSP-LOADED SLNS ON *in vitro* DIURETIC ACTIVITY

Sample	Conc. (µg/mL)	Mean ± SD			DA (Na^+)	DA (K^+)	DA (Cl^-)	DI (Na^+)	DI (K^+)	DI (Cl^-)
		Na^+	K^+	Cl^-						
Control	–	0.20 ± 0.12	0.15 ± 0.11	0.18 ± 0.13	–	–	–	–	–	–
Standard	50	0.32 ± 0.14	0.28 ± 0.21	0.30 ± 0.14	1.60	1.87	1.67	1.00	1.00	1.00
	75	0.40 ± 0.11	0.35 ± 0.13	0.38 ± 0.12	2.00	2.33	2.11	1.00	1.00	1.00
	100	0.50 ± 0.08	0.42 ± 0.14	0.45 ± 0.13	2.50	2.80	2.50	1.00	1.00	1.00
Extract	50	0.28 ± 0.09**	0.24 ± 0.09*	0.26 ± 0.15**	1.40	1.60	1.44	0.88	0.86	0.87
	75	0.35 ± 0.11**	0.30 ± 0.11*	0.33 ± 0.16**	1.75	2.00	1.83	0.88	0.86	0.87
	100	0.43 ± 0.12***	0.37 ± 0.18*	0.40 ± 0.14**	2.15	2.47	2.22	0.86	0.88	0.89
SLNs (GSP4)	50	0.34 ± 0.15**	0.30 ± 0.17**	0.32 ± 0.13**	1.70	2.00	1.78	1.06	1.07	1.07
	75	0.45 ± 0.17**	0.38 ± 0.11**	0.41 ± 0.17**	2.25	2.53	2.28	1.13	1.09	1.08
	100	0.55 ± 0.11***	0.46 ± 0.17**	0.48 ± 0.16**	2.75	3.07	2.67	1.10	1.10	1.07

All the studies carried out in triplicate and datas are represented in Mean ± SD. $^{**}p \leq 0.05$ considered as significant in comparison to control group, $^{*}p \geq 0.05$ considered as less significant in comparison to control group.

the SAIF, Indian Institute of Technology Bombay, Mumbai, India, for providing ESEM, TEM, FTIR, TGA and DTA analysis facilities. The authors also sincerely acknowledge the CIF, Lovely Professional University, Phagwara, India, for providing particle size and zeta potential analysis facilities.

CONFLICT OF INTEREST

The authors declare that there is no conflict of interests regarding the publication of this article.

DECLARATION OF AI-ASSISTED TECHNOLOGIES

During the preparation of this manuscript, the authors used an AI-assisted tool(s) to improve the language and no data, results or scientific conclusions were generated by AI. All analyses, interpretations and conclusions are the authors' own. The authors reviewed and edited the content and take full responsibility for the published work.

REFERENCES

1. R.K. Goyal, J. Singh and H. Lal, *Indian J. Med. Sci.*, **57**, 408 (2003); https://doi.org/10.1055/s-0041-173542
2. V. Sharma, M. Thakur, N.S. Chauhan and V.K. Dixit, *Pharm. Biol.*, **44**, 508 (2018); https://doi.org/10.1080/13880200600897556
3. S. Alok, S. K. Jain, A. Verma, M. Kumar, A. Mahor and M. Sabharwal, *Asian Pac. J. Trop Dis.*, 3, 242 (2013); https://doi.org/10.1016/S2222-1808(13)60049-3
4. M. Gupta and B. Shaw, *Iran. J. Pharm. Res.*, **10**, 167 (2011).
5. J. Jeevanandam, A. Barhoum, Y.S. Chan, A. Dufresne and M.K. Danquah, *Beilstein J. Nanotechnol.*, **9**, 1050 (2018); https://doi.org/10.3762/bjnano.9.98
6. S. Sangeetha, N. Geetha and R. Kumar, *Mater. Lett.*, **282**, 128794 (2021); https://doi.org/10.1016/j.matlet.2020.128794
7. S. Akhtar, A. K. Gupta, B. Naik, V. Kumar, R. Ranjan, A.K. Jha, M.A. Rather and S. Rustagi, *Food Chem. Adv.*, **4**, 100689 (2024); https://doi.org/10.1016/j.focha.2024.100689
8. G. Sharma, A.R. Sharma, J.S. Nam, G.P.C. Doss, S.S. Lee and C. Chakraborty, *J. Nanobiotechnology*, **13**, 74 (2015); https://doi.org/10.1186/s12951-015-0136-y
9. S. Iravani, *Green Chem.*, **13**, 2638 (2011); https://doi.org/10.1039/c1gc15386b
10. S.H. Rasheed, R.K. Vakkalagadda, S. Mustak and S. Sen, *Pharmacogn. Res.*, **16**, 161 (2023); https://doi.org/10.5530/pres.16.1.21
11. N. Chaudhary, M.B. Siddiqui and S. Khatoon, *Indian J. Tradit. Knowl.*, **13**, 543 (2014); https://doi.org/10.14233/ajchem.2024.28919
12. L.B.D.C. Araújo, S.L. Silva, M.A.M. Galvão, M.R.A. Ferreira, E.L. Araújo, K.P. Randau and L.A.L. Soares, *Rev. Bras. Farmacogn.*, **23**, 736 (2013); https://doi.org/10.1590/S0102-695X2013000500004
13. S. Sen, B. De and T.S. Easwari, *Asian J. Chem.*, **26**, 6616 (2014); https://doi.org/10.14233/ajchem.2014.17003
14. K. Das, S.M.B. Asdaq, M.S. Khan, S. Amrutha, M. Alhomrani, A. Alamri, W.F. Alsanie, A. Bhaskar, G.C. Shree and P. Harshitha, *J. King Saud Univ. Sci.*, **34**, 102261 (2022); https://doi.org/10.1016/j.jksus.2022.102261
15. D.S.H.S. Peiris, D.T.K. Fernando, S.P.N.N. Senadeera and C.B. Ranaweera, *Asian J. Res. Biochem.*, **15**, 37 (2025); https://doi.org/10.9734/ajrb/2025/v15i2365.
16. R. Hirani, *IP Int. J. Compr. Adv. Pharmacol.*, **8**, 86 (2023); https://doi.org/10.18231/j.ijcaap.2023.015
17. K. Kuotsu, K.M. Karim, A.S. Mandal, N. Biswas, A. Guha, S. Chatterjee and M. Behera, *J. Adv. Pharm. Technol. Res.*, **1**, 374 (2010); https://doi.org/10.4103/0110-5558.76435
18. H. Refai, D. Hassan and R. Abdelmonem, *Drug Deliv.*, **24**, 278 (2017); https://doi.org/10.1080/10717544.2016.1247925
19. S. Bhattacharjee, *J. Control. Release*, **235**, 337 (2016); https://doi.org/10.1016/j.jconrel.2016.06.017.
20. A.R. Gardouh, *J. Pharm. Res. Int.*, **3**, 326 (2013); https://doi.org/10.9734/BJPR/2013/2770
21. J.M. Rami, C.D. Patel, C.M. Patel and M.V. Patel, *Mater. Today Proc.*, **43**, 655 (2021); https://doi.org/10.1016/j.matpr.2020.12.554
22. G.P. Kumar and P. Rajeshwarrao, *Acta Pharm. Sin. B*, **1**, 208 (2011); https://doi.org/10.1016/j.apsb.2011.09.002
23. S. Sen, K. Swathi, K.D. Vishwanath, B. Ravindar, M. Chaitanya, S. Cherukupally, S. Tejasree and H.V. Santhoshi Allu, *Pharmacogn. Res.*, **16**, 887 (2024); https://doi.org/10.5530/pres.16.4.101
24. V G, Kothapalli, M. A. Vasanthan, *Cureus*, **16**, e68339 (2024); https://doi.org/10.7759/cureus.68339
25. A. Naim, A.M. Farooqui, M.I. Badruddeen, M.I. Khan, J. Akhtar, A. Ahmad, S. Ashique and A. Islam, *Front. Neurol.*, **17**, 1792829 (2026); https://doi.org/10.3389/fneur.2026.1792829